

Effects of uniform electric fields on intracellular calcium transients in single cardiac cells

VINOD SHARMA AND LESLIE TUNG

Department of Biomedical Engineering, The Johns Hopkins University, Baltimore, Maryland 21205

Received 9 April 2001; accepted in final form 14 September 2001

Sharma, Vinod, and Leslie Tung. Effects of uniform electric fields on intracellular calcium transients in single cardiac cells. *Am J Physiol Heart Circ Physiol* 282: H72–H79, 2002.—Although intracellular calcium ($[Ca^{2+}]_i$) transients in cardiac cells have been well studied in the uniformly polarized cell membrane, how these transients are modified during field stimulation when the cell membrane is nonuniformly polarized has not been investigated. In this study we characterized the effects of uniform field stimuli on $[Ca^{2+}]_i$ transients in isolated guinea pig cardiac cells. Single guinea pig cells were enzymatically isolated, loaded with the $[Ca^{2+}]_i$ fluorescent indicator fluo-3, and stimulated along their longitudinal axes with S1 or S1-S2 (S1-S2 = 50 ms) pulses. The fluorescence signals were recorded simultaneously from up to 12 sites along the cell length using a multisite mapping system. S1 pulse, applied during the resting phase of the action potential, induced $[Ca^{2+}]_i$ transients that had an earlier onset at the anodal-facing end, suggesting that $[Ca^{2+}]_i$ gradients ($\nabla[Ca^{2+}]_i$) develop during the rising phase of the $[Ca^{2+}]_i$ transients. With the assumption that the peak change in $[Ca^{2+}]_i$ is 980 nM, $\nabla[Ca^{2+}]_i$ was estimated to be ~ 3.4 nM/ μ m in the anodal half of the cell for a nominal 10 V/cm field and negligible in the cathodal half. The S2 pulse that was applied during the plateau of the action potential also perturbed the $[Ca^{2+}]_i$ transients and produced $[Ca^{2+}]_i$ gradients directed from the center to either end of the cell. Mean $\nabla[Ca^{2+}]_i$ in the anodal half of the cell (~ 4.2 nM/ μ m) was found to be statistically higher than in the cathodal half (~ 2.8 nM/ μ m).

cardiac electrophysiology; fluo-3; optical mapping; guinea pig

IN THE HEART Ca^{2+} plays a crucial role in transducing electrical excitation into muscle contraction. The depolarization causes a rise in intracellular Ca^{2+} concentration ($[Ca^{2+}]_i$) and results in muscle contraction. In addition, $[Ca^{2+}]_i$ affects diverse cellular processes, including gating of numerous ion channels. Because Ca^{2+} is an extremely important ion in cellular physiology, considerable effort has been spent to understand the many factors that influence $[Ca^{2+}]_i$ dynamics (4).

Experiments using fluorescent $[Ca^{2+}]_i$ indicators (e.g., fura 2, indo-1, and fluo-3) and pharmacological interventions have revealed a great deal about the $[Ca^{2+}]_i$ dynamics in a uniformly polarized cell membrane. Depolarization-induced influx of Ca^{2+} occurs predominantly via sarcolemmal L-type Ca^{2+} channels

and induces rapid and synchronous release of Ca^{2+} from the sarcoplasmic reticulum (SR) via the mechanism of calcium-induced calcium release (CICR) (14). As a result, $[Ca^{2+}]_i$ increases uniformly over the entire cell length (28). For example, in the guinea pig, $[Ca^{2+}]_i$ increases from a resting value of ~ 120 nM to a peak value of $\sim 1,100$ nM during an action potential (7). The Ca^{2+} released from the SR contributes the majority of $[Ca^{2+}]_i$ (10, 26), and in the guinea pig the SR contribution is ~ 70 – 80% (5, 13, 15). The $[Ca^{2+}]_i$ transient reaches its peak value within ~ 35 ms from the onset and declines thereafter with the majority of Ca^{2+} returned to the SR by SR Ca^{2+} ATPase (SERCA) (6, 26). The sarcolemmal Na^+/Ca^{2+} exchanger also extrudes a small amount of Ca^{2+} from the cell, which is equivalent to the amount of Ca^{2+} entered via L-type Ca^{2+} channels (5, 8).

Because the Ca^{2+} entry via L-type Ca^{2+} channels is membrane voltage dependent, it is possible that during field stimulation, when the cell is nonuniformly polarized and different regions of the cell experience very different transmembrane voltages (11, 24, 32), spatial differences in Ca^{2+} current and therefore $[Ca^{2+}]_i$ can exist. To date no experimental studies have addressed the above hypothesis. Thus the aim of this study was to characterize the $[Ca^{2+}]_i$ transients in adult guinea pig ventricular cells field stimulated at rest and during the plateau phase of the action potential by using the fluorescent indicator fluo-3 and a high resolution multisite optical mapping system. We show that external fields can indeed induce spatial inhomogeneities and gradients in $[Ca^{2+}]_i$ both during rest and the plateau.

METHODS

Single ventricular myocytes were enzymatically isolated from whole hearts of adult male guinea pigs (Hartley strain, weight 200–300 g) as follows. The animals were anesthetized with an intraperitoneal injection of pentobarbital sodium (0.1 ml/100 g, Abbott Laboratories; North Chicago, IL) combined with 0.1–0.3 ml of heparin to minimize clotting. Once the animal failed to respond to the paw pinch test, its chest was quickly opened via a radical medial thoracotomy. The heart was quickly excised, mounted on a Langendorff column, and perfused retrogradely through the aorta. The enzymatic dissociation was performed using the following sequence of

Address for reprint requests and other correspondence: L. Tung, Dept. of Biomedical Engineering, The Johns Hopkins Univ., 720 Rutland Ave., Baltimore, MD 21205 (E-mail: ltung@bme.jhu.edu).

The costs of publication of this article were defrayed in part by the payment of page charges. The article must therefore be hereby marked "advertisement" in accordance with 18 U.S.C. Section 1734 solely to indicate this fact.

solutions, all of which were oxygenated and maintained at 37°C: 1) 1.8 mM Ca^{2+} Tyrode's solution for 5 min; 2) Ca^{2+} -free Tyrode's solution for 7 min; 3) 50 ml Ca^{2+} -free Tyrode's solution with 0.25 mg/ml protease (type XIV, Sigma; St. Louis, MO), 0.3 mg/ml collagenase (Worthington Biochemical; Freehold, NJ), and 1 mg/ml bovine serum albumin (type V, Sigma) for 7 min; and 4) Ca^{2+} -free Tyrode's solution for 5 min. After perfusion the ventricles were chopped, gently stirred, and filtered to obtain single cells.

Cells were loaded with the $[\text{Ca}^{2+}]_i$ -sensitive dye fluo-3 by exposure to a 3 μM solution of cell-permeable fluo-3 AM (Molecular Probes; Eugene, OR) for 30–50 min. Fluo-3 loading solution was prepared by a 1,000-fold dilution of a 3 mM stock solution in dimethyl sulfoxide containing 20% wt/wt of Pluronic 127 (Molecular). After dye loading was completed, the cells were allowed to deesterify for 20–30 min and thereafter used for experimentation immediately.

During all experiments the cells were continuously superfused with normal Tyrode's solution maintained at 34–36°C. The floor of the experimental chamber consisted of a 0.17-mm thick, 22-mm diameter glass coverslip, which was cleaned thoroughly with sulfuric acid before each session. This allowed a majority of the cells to adhere firmly to the coverslip, thus minimizing the motion artifact in the fluorescence recordings. The composition of the Tyrode's solution (in mM) was 135 NaCl, 5.4 KCl, 1 MgCl_2 , 0.33 NaH_2PO_4 , 5 HEPES, 1.8 CaCl_2 , and 5 glucose (adjusted to pH 7.4 with NaOH). The longitudinal axis of the cell under investigation was aligned with the field direction, and the cell was paced at 1 Hz using 5-ms duration (S1) field pulses. The experiments were performed with an S1 pulse only or with a combination of S1 and S2 pulses in which the S2 pulse (20 ms in duration) was applied 50 ms after the onset of the S1 pulse. The S1 pulse caused the cell to elicit $[\text{Ca}^{2+}]_i$ transient so that S2 was applied during the plateau phase of the $[\text{Ca}^{2+}]_i$ transient. Reversing the polarity of field electrodes reversed the field direction. The field directed from left to right is defined as positive (e.g., Fig. 3).

The experimental setup was assembled around an inverted microscope (Diaphot-TMD, Nikon). The light from a 150-W Xenon arc lamp (Opti Quip; Highland Mills, NY) was coupled into the epiillumination pathway of the microscope to excite the dye. The exposure time was controlled using an electronic shutter (Vincent Associates; Rochester, NY). The specifications of the optical filters used for recording $[\text{Ca}^{2+}]_i$ signals were as follows: excitation filter (ExF): 450–490 nm, dichroic (D): 510 nm, and emission filter (EmF): 520–560 nm. The fluorescence image of the cell was projected onto a bundle of 149 hexagonally packed plastic optical fibers. At $\times 60$ magnification used for this study, each 1-mm diameter optical fiber collected fluorescence from a 17- μm spot in the specimen plane. The fluorescence signals were mapped along the cell length using up to 12 fibers. The fluorescence signals from these fibers were fed into an equal number of signal detection and conditioning circuits. The recording duration had two different settings: 400 and 150 ms. The longer 400-ms duration (at a sampling rate of 5 kHz per channel) allowed recording of complete transients but restricted the total number of exposures to one to three because dye photobleaching rapidly deteriorated the quality of signals. The shorter 150-ms duration (at a sampling rate of 10 kHz per channel) enabled up to 12 exposures from a cell. The baseline fluorescence level with the shorter recording duration essentially remained the same for two consecutive recordings and facilitated their comparison. The $[\text{Ca}^{2+}]_i$ signals from various sites were normalized to the signal level ~ 30 ms after the onset of the transients. For all experiments, the S1 field

amplitude ranged from 5 to 20 V/cm and S2 amplitude from 8 to 40 V/cm.

To allow comparison of results obtained from cells of varying lengths, the field amplitudes were scaled by $L/120$, where L was the length (in μm) of the cell being stimulated. The scaled amplitude represents an equivalent electric field for a nominal 120- μm long cell, which is the average length for a guinea pig ventricular cell (30).

The statistical correlation between any two parameters was determined by calculating Pearson's correlation coefficient (R) and conducting a two-tailed Student's t -test for rejecting the null hypothesis that the slope of the best fit line was zero, and that the parameters were not correlated. Whenever applicable a two-tailed, Student's paired t -test was used to compare the means of various data sets. Values of $P < 0.05$ were considered to be significant.

RESULTS

Typical $[\text{Ca}^{2+}]_i$ transients. Figure 1A shows the image of a cell for which $[\text{Ca}^{2+}]_i$ signals were recorded using longer (400 ms) exposure time. The $[\text{Ca}^{2+}]_i$ transients were recorded from eight sites on the cell in response to one of the S1 (~ 7 V/cm) pacing pulses and are shown superimposed in Fig. 1B. The S1 pulse is shown beneath the $[\text{Ca}^{2+}]_i$ transients. Because the cell was adhered firmly to the glass coverslip, the motion artifact during the initial ~ 100 ms of the transients was negligible. Thereafter, a slight motion artifact was present, and the $[\text{Ca}^{2+}]_i$ signals from the various sites showed some spread (Fig. 1B). The mean duration (computed by measuring the duration between the 10% values of the peak $[\text{Ca}^{2+}]_i$ for each site and taking the average) of the $[\text{Ca}^{2+}]_i$ transients shown in Fig. 1B was ~ 270 ms, and the time to reach the peak from the onset of the transient was ~ 40 ms. The duration of $[\text{Ca}^{2+}]_i$ transients were measured for 18 cells with 400-ms

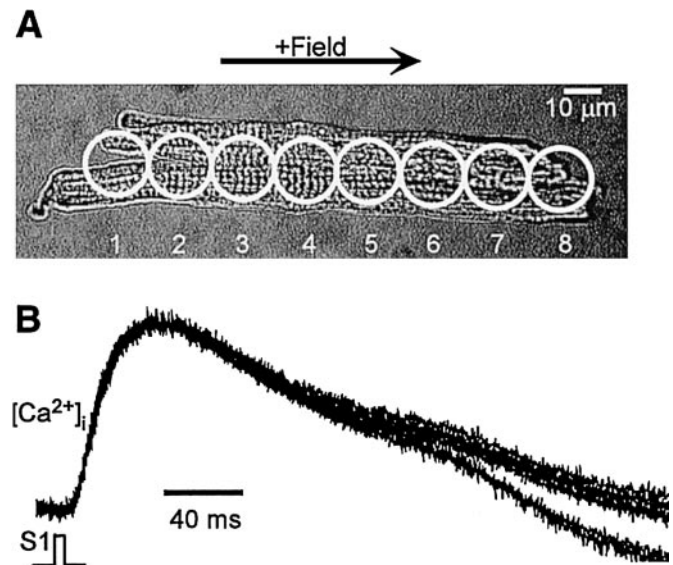


Fig. 1. Typical complete intracellular Ca^{2+} ($[\text{Ca}^{2+}]_i$) transients. Cell shown in A was stimulated with an S1 field pulse of ~ 7 V/cm in the indicated direction, and $[\text{Ca}^{2+}]_i$ transients were recorded for a duration of 400 ms from 8 sites on the cell. $[\text{Ca}^{2+}]_i$ transients from all sites are shown superimposed in B and illustrate the recordings were motion-artifact free for at least the initial ~ 100 ms.

recording duration and was found to be 245 ± 42 (means \pm SD) ms. The time to peak of the $[Ca^{2+}]_i$ transient was measured for 26 cells with both short (150 ms) and long (400 ms) recording durations and was found to be 34 ± 11 ms.

Effect of ryanodine and nifedipine. Figure 2 shows examples of the effect of $5 \mu M$ nifedipine (a sarcolemmal Ca^{2+} channel blocker) and $2 \mu M$ ryanodine (a blocker of SR Ca^{2+} -release channel), respectively. Fig-

ure 2 also shows control recordings obtained before drug exposure (*left*) and recordings obtained ~ 5 min after perfusion with a solution containing the drug. Consistent with previously published reports (2), both of these interventions were able to strongly suppress the signals recorded from fluo-3-loaded cells, thus establishing that the recorded signals were indeed $[Ca^{2+}]_i$ sensitive. Similar results were obtained for two other cells (each for nifedipine and ryanodine). Small residual transients were observed in the presence of nifedipine, possible causes of which are mentioned in DISCUSSION. The amplitude of $[Ca^{2+}]_i$ transients in the presence of ryanodine was ~ 10 – 15% of the control (Fig. 2B), suggesting that L-type Ca^{2+} current constitutes for ~ 10 – 15% of the $[Ca^{2+}]_i$ transient in guinea pig.

Effect of S1 on $[Ca^{2+}]_i$ transients. The $[Ca^{2+}]_i$ transients were recorded from eight sites on the cell shown in Fig. 3A for positive ($S1 = +10$ V/cm) and negative ($S1 = -11$ V/cm) field directions and are shown in Fig. 3B. For both field directions, the $[Ca^{2+}]_i$ transients from the various sites were not completely synchronous. For the positive S1 pulse, the $[Ca^{2+}]_i$ signal from *site 1* was the fastest to rise, and $[Ca^{2+}]_i$ signal from *site 8* was the slowest (Fig. 3B, *middle row*). On field reversal this trend was reversed, and the signal from *site 8* was the fastest to rise (Fig. 3B, *bottom row*). These asynchronous signals imply that the $[Ca^{2+}]_i$ was nonuniform along the cell length during the rising phase of the transients, and thus gradients in $[Ca^{2+}]_i$ ($\nabla[Ca^{2+}]_i$) were developed. To estimate $\nabla[Ca^{2+}]_i$ the normalized change in $[Ca^{2+}]_i$ ($\Delta[Ca^{2+}]_{iN}$) was measured for the various sites along the cell length at a single instant corresponding to $\sim 50\%$ activation point (thick vertical line in Fig. 3B). $\Delta[Ca^{2+}]_{iN}$ was obtained by normalizing the change in $[Ca^{2+}]_i$ from the resting value ($\Delta[Ca^{2+}]_i$) to the peak change ($\Delta[Ca^{2+}]_{iO}$) (Fig. 3C, *inset*). From Fig. 3C it is clear that both $\Delta[Ca^{2+}]_{iN}$ and $\nabla[Ca^{2+}]_i$ were nonuniform along the cell length (apparent from nonconstancy of the relation) with large $[Ca^{2+}]_i$ gradients existing in the regions of the cell facing the anode. On field reversal, the trend in $\Delta[Ca^{2+}]_{iN}$ and $\nabla[Ca^{2+}]_i$ was reversed, thus establishing that these patterns indeed depended on field direction and were not the result of intrinsic heterogeneities in the cell. Assuming $\Delta[Ca^{2+}]_{iO}$ to be ~ 980 nM for a typical guinea pig cell (7), $\nabla[Ca^{2+}]_i$ values in the anodal half of the cell shown in Fig. 3A were estimated to be 4.2 and 6.3 nM/ μm for the positive and negative S1 pulses, respectively (refer to Fig. 3C, *bottom*, for method of computing $\nabla[Ca^{2+}]_i$).

An inspection of the superimposed $[Ca^{2+}]_i$ transients in Fig. 3B reveals that the $[Ca^{2+}]_i$ transients from all sites were delayed as a group from the onset of the S1 pulse. This time delay (t_d) measured from the onset of S1 pulse was ~ 7.5 ms for the transients shown in Fig. 3B. Note that a similar delay is present in the recordings shown in Fig. 1B as well, which was measured to be ~ 8 ms.

Results similar to those described above were obtained for 26 cells (114 S1 stimuli) and are summarized

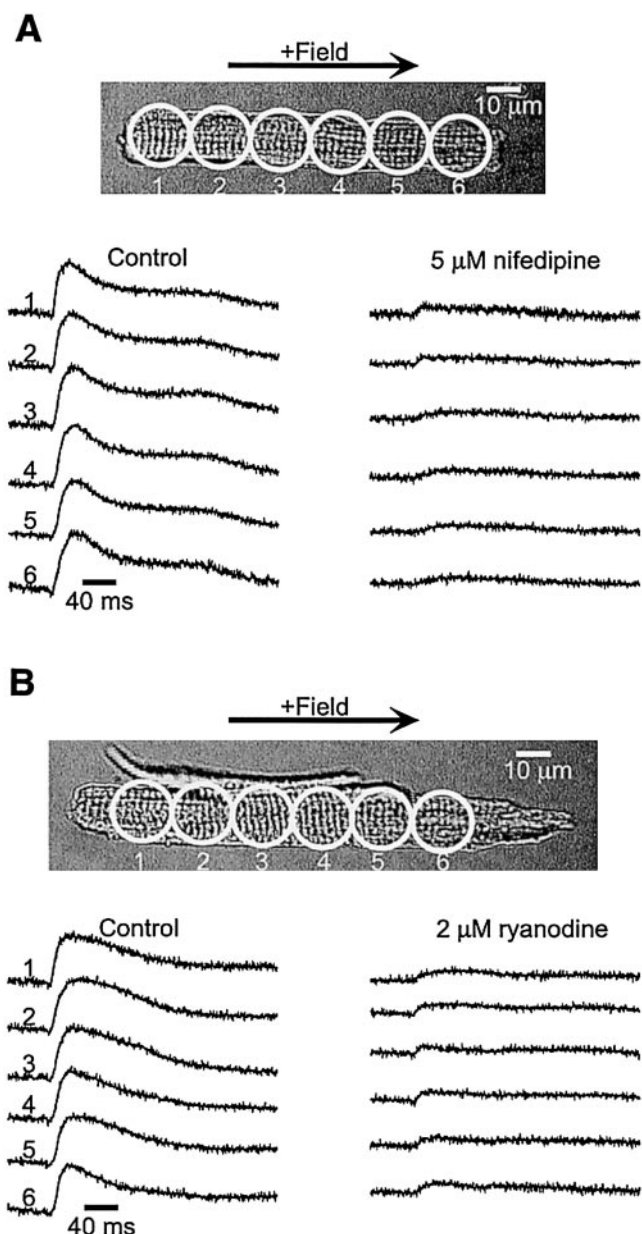


Fig. 2. Effect of nifedipine and ryanodine on $[Ca^{2+}]_i$ transients. A: cell stimulated with an S1 field pulse in the indicated direction. $[Ca^{2+}]_i$ transients recorded from 6 sites in normal Tyrode's solution (control, *left*) and in presence of $5 \mu M$ nifedipine (*right*) are shown below the cell. Nifedipine abolished $[Ca^{2+}]_i$ transients. B: shows another cell for which $[Ca^{2+}]_i$ transients were recorded in the absence (control, *left*) and presence of $2 \mu M$ ryanodine (*right*). Ryanodine suppressed $[Ca^{2+}]_i$ transients, and amplitude of the residual transients was $\sim 10\%$ of control level.

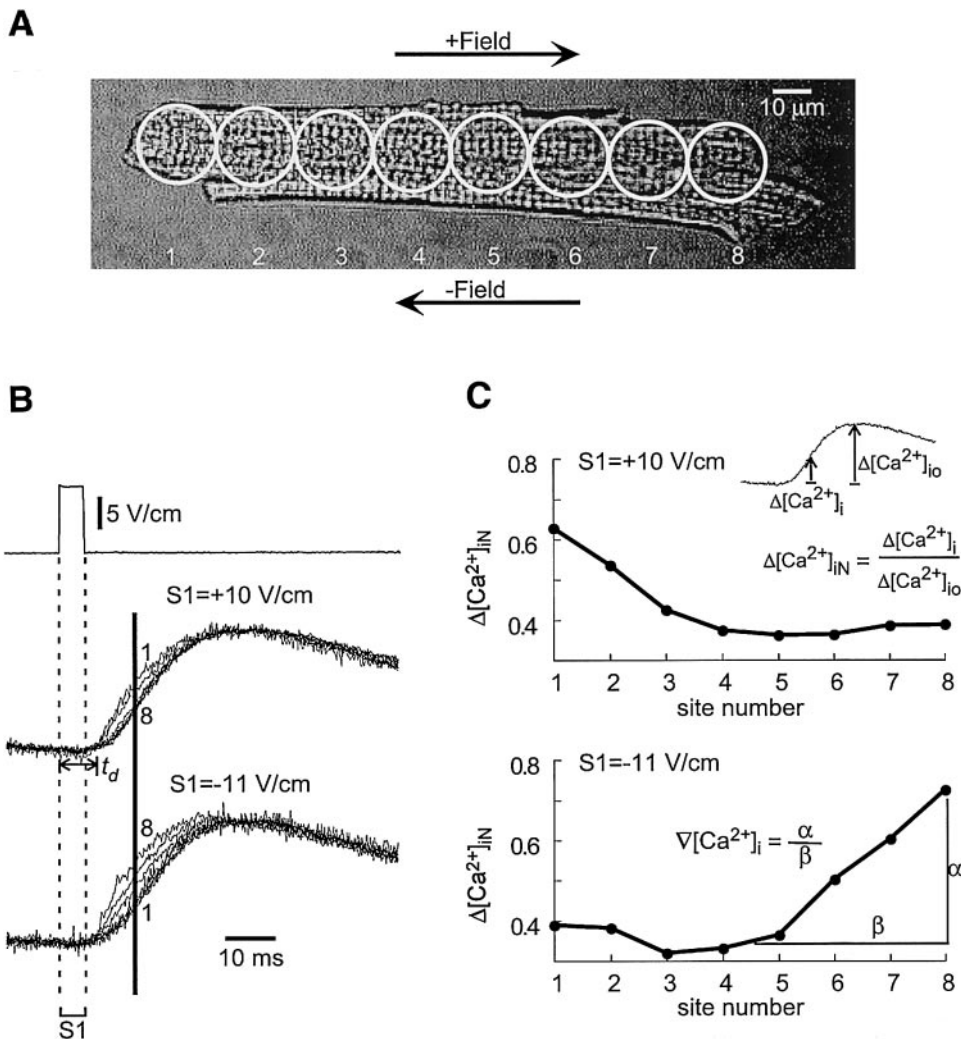


Fig. 3. Effect of S1 pulse. *A*: cell that was stimulated with positive and negative S1 pulses; *B*: corresponding $[Ca^{2+}]_i$ transients superimposed from all 8 sites. For both field pulses, $[Ca^{2+}]_i$ transients from all sites were not completely synchronous. In *B*, *top* shows the positive S1 pulse; *middle* shows that for this S1 pulse of +10 V/cm, the $[Ca^{2+}]_i$ signal from *site 1* was the fastest to rise, and the signal from *site 8* was the slowest; and *bottom* shows that on field reversal, this trend in the onset of $[Ca^{2+}]_i$ signals was reversed. The pair of vertical dashed lines spanning the duration of the S1 pulse help to discern the temporal relationship between the S1 pulse and $[Ca^{2+}]_i$ transients. Onset of $[Ca^{2+}]_i$ transients from all sites as a group was delayed from the make of the S1 pulse by a time duration (t_d), which was ~ 7.5 ms for both positive and negative S1 pulses. Change in $[Ca^{2+}]_i$ relative to the resting level ($\Delta[Ca^{2+}]_i$) was measured during rising phase of the transients at the time indicated by the thick line in *B*. $\Delta[Ca^{2+}]_i$ was normalized to the peak value ($\Delta[Ca^{2+}]_{i0}$) of $\Delta[Ca^{2+}]_i$ (*C*, *inset*), and the resulting normalized change ($\Delta[Ca^{2+}]_{iN}$) is plotted in *C* for positive S1 (*top*) and negative S1 (*bottom*) pulses. Gradient in $[Ca^{2+}]_i$ ($\nabla[Ca^{2+}]_i = \alpha/\beta$) in the anodal half of the cell was computed as illustrated in *C*, *bottom*, and was estimated to be 4.2 and 6.3 nM/ μ m for the positive and negative S1 pulses, respectively (see text for additional details).

in Fig. 4. Figure 4A shows that $\nabla[Ca^{2+}]_i$ in the anodal half of the cell increased monotonically with the S1 amplitude ($R = 0.46$, $P < 0.001$), and $\nabla[Ca^{2+}]_i$ is estimated to be ~ 3.4 nM/ μ m for a nominal field of ~ 10 V/cm. $\nabla[Ca^{2+}]_i$ in the cathodal half of the cell was negligible. Figure 4B shows that t_d decreased monotonically with the S1 amplitude ($R = 0.39$, $P < 0.001$).

Effect of S2 on $[Ca^{2+}]_i$ transients. Figure 5 illustrates the effect of the S2 pulse on the $[Ca^{2+}]_i$ transients. The onset of the S2 pulse occurred 50 ms after the break of the S1 pulse. The recordings were obtained from eight sites on the cell shown in Fig. 5A, first in response to an S1 pulse (+8 V/cm) only, and then in response to a pair of S1-S2 pulses (S1 = +8 V/cm, S2 = +29 V/cm). The recordings from the various sites in the absence and presence of the S2 pulse are shown superimposed in Fig. 5B. The bottommost row in Fig. 5B shows superimposed recordings from all sites obtained in response to the S1-S2 pair. The nonoverlapping behavior of these recordings suggests that the S2 caused nonuniformities in $[Ca^{2+}]_i$ along the cell length and produced $[Ca^{2+}]_i$ gradients. The S2-induced change in the $[Ca^{2+}]_i$ ($\Delta[Ca^{2+}]_i$) was measured at the end of S2 pulse relative to the $[Ca^{2+}]_i$ at the same time recorded with

S1 pulse only (Fig. 5C, *inset*). Similar to the case of the S1 pulse described above, $\Delta[Ca^{2+}]_i$ was normalized to the peak of the $[Ca^{2+}]_i$ transient ($\Delta[Ca^{2+}]_{i0}$), and the result ($\Delta[Ca^{2+}]_{iN}$) is shown in Fig. 5C, *top*. On field reversal of S1 and S2, a similar behavior of $\Delta[Ca^{2+}]_{iN}$ along the cell length was observed (Fig. 5C, *bottom*). These results suggest that during the S2 pulse, intracellular calcium gradients develop from the center to either end of the cell. In Fig. 5C the $\nabla[Ca^{2+}]_i$ values in the anodal and cathodal halves of the cell were found to be 5.6 and 5.2 nM/ μ m, respectively, for the positive fields, and 7.7 and 5.0 nM/ μ m, respectively, for the negative fields. Results similar to those described above were obtained for $n = 12$ cells (24 S1-S2 stimuli; S2 = 25 ± 6 V/cm). The $\nabla[Ca^{2+}]_i$ in the anodal half (4.2 ± 2.2 nM/ μ m) of the cell was found to be statistically higher than in the cathodal half (2.8 ± 1.6 nM/ μ m) ($P < 0.03$).

A closer inspection of Fig. 5B reveals the details of the time course of the S2-induced $[Ca^{2+}]_i$ perturbation along the cell length. The $[Ca^{2+}]_i$ transients deflected downward at the onset of S2 pulse at both the anodal and cathodal ends, and a surge in $[Ca^{2+}]_i$ was observed at both ends of the cell upon S2 termination. The surge

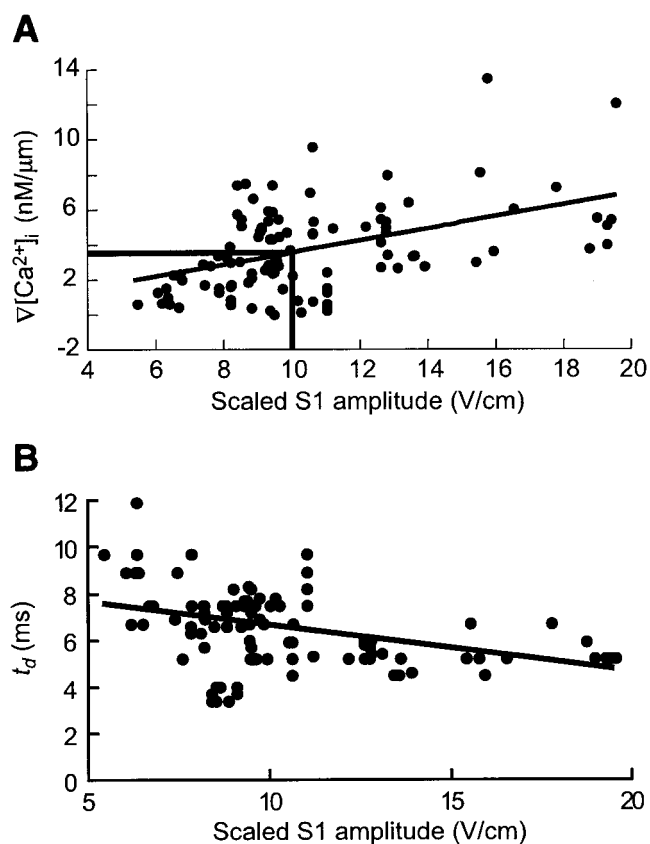


Fig. 4. Summary of S1 pulse results. *A*: $\nabla[\text{Ca}^{2+}]_i$ versus scaled S1 amplitude for 26 cells (114 S1 stimuli). $\nabla[\text{Ca}^{2+}]_i$ increased monotonically with the S1 pulse amplitude ($R = 0.46$, $P < 0.001$). Intersection of horizontal and vertical lines indicates that $\nabla[\text{Ca}^{2+}]_i$ was ~ 3.4 $\text{nM}/\mu\text{m}$ for a nominal 10 V/cm S1 pulse. *B*: t_d plotted against scaled S1 amplitude. The t_d decreased monotonically with an increase in S1 amplitude ($R = 0.39$, $P < 0.001$).

was slightly larger at the cathodal end (compare signals from *sites 1* and *8* in Fig. 5*B*). In the central region of the cell (*sites 4* and *5*), a slight increase in $[\text{Ca}^{2+}]_i$ was observed at the onset of the S2 pulse. These observations were typical of the S2-induced perturbation of $[\text{Ca}^{2+}]_i$.

DISCUSSION

In this study we used a multisite optical mapping system to record $[\text{Ca}^{2+}]_i$ transients along the lengths of isolated guinea pig ventricular myocytes and characterized the effects of uniform electric fields on $[\text{Ca}^{2+}]_i$ transients. We show that consistent with our hypothesis, an externally applied electric field can induce spatial heterogeneities in an isolated cardiac cell during both rest and the action potential plateau. To the best of our knowledge this is the first study showing subcellular scale calcium gradients in a nonuniformly polarized cardiac cell during field stimulation. Specifically, we show that a 5-ms duration S1 field pulse applied at rest results in an asynchronous rise in $[\text{Ca}^{2+}]_i$ along the cell length and induces spatial $\nabla[\text{Ca}^{2+}]_i$. $\nabla[\text{Ca}^{2+}]_i$ estimated during the midpoint of the rising phase of the $[\text{Ca}^{2+}]_i$ transients is large in the

anodal half of the cell (Fig. 3*C*), increases monotonically with the S1 amplitude (Fig. 4*A*), and has a value of ~ 3.4 $\text{nM}/\mu\text{m}$ for a nominal 10 V/cm field. The S2 field pulse applied during the plateau also perturbs $[\text{Ca}^{2+}]_i$ and results in $[\text{Ca}^{2+}]_i$ gradients along the cell length (Fig. 5*B*). $\nabla[\text{Ca}^{2+}]_i$ during the plateau is directed from the center to either end of the cell (Fig. 5*C*) and on average is greater in the anodal half than in the cathodal half (4.2 and 2.8 $\text{nM}/\mu\text{m}$, respectively, for an S2 pulse of ~ 25 V/cm). As we discuss below, this is consistent with the notion that the diffusion of intracellular Ca^{2+} is a relatively slow process.

The field-induced change in $[\text{Ca}^{2+}]_i$ can be $>20\%$ (Fig. 5*C*). The change in $[\text{Ca}^{2+}]_i$ and its relatively large magnitude are likely the result of: 1) field modulation of the L-type Ca^{2+} current, which directly contributes about 20–30% of the Ca^{2+} transient in guinea pig (5, 15), and 2) further amplification of the modulated Ca^{2+} current in the form of CICR from the SR (9). Consistent with the latter hypothesis, $[\text{Ca}^{2+}]_i$ transients were suppressed by the interventions that blocked either the sarcolemmal Ca^{2+} current or SR Ca^{2+} release (Fig. 2). The small residual transients in the presence of nifedipine (Fig. 2*A*) are probably because of one or more of the following: 1) incomplete block of L-type Ca^{2+} current, 2) T-type Ca^{2+} current that is not blocked by nifedipine, 3) reverse mode $\text{Na}^+/\text{Ca}^{2+}$ exchanger acting to produce a small transient or serving as a weak trigger for Ca^{2+} release from the SR in the depolarized regions of the cell (25).

The pattern of S1- and S2-induced gradients can be explained in terms of what is known about voltage gating and the current-voltage (I - V) relation of the L-type Ca^{2+} channel and the relationship between Ca^{2+} current and Ca^{2+} release from the SR. The I - V relation of the L-type Ca^{2+} channel has a characteristic bell shape with peak inward current occurring at ~ 10 mV that declines to near-zero values at $+60$ and -60 mV (18, 22, 23, 29). Some studies have found SR Ca^{2+} release to vary linearly with Ca^{2+} current (9), although others have found more complicated relations (10, 23). However, irrespective of the details of this relation, it is clear that the qualitative changes in $[\text{Ca}^{2+}]_i$ in response to changes in the transmembrane potential will be governed by the I - V relation of the Ca^{2+} current.

It has been well established experimentally that single cardiac cells undergo nonuniform polarization in response to a uniform electric field stimulus (11, 24). Thus the S1 field pulse applied at rest hyperpolarizes the end of the cell facing the anode and depolarizes the end facing the cathode. Furthermore, our experiments reveal that $[\text{Ca}^{2+}]_i$ rises faster at the anodal end (Fig. 3*B*). Because the resting potential (approximately -90 mV) is situated at the leftmost extreme of the bell-shaped I - V relation of the L-type Ca^{2+} current, the S1 pulse will activate a large inward Ca^{2+} current at the cell end facing the cathode but a negligible current at the end facing the anode. This should result in a large $[\text{Ca}^{2+}]_i$ transient at the cathodal, but not the anodal, end. However, because activation of the cell likely occurs during the S1 pulse, the nonuniform membrane

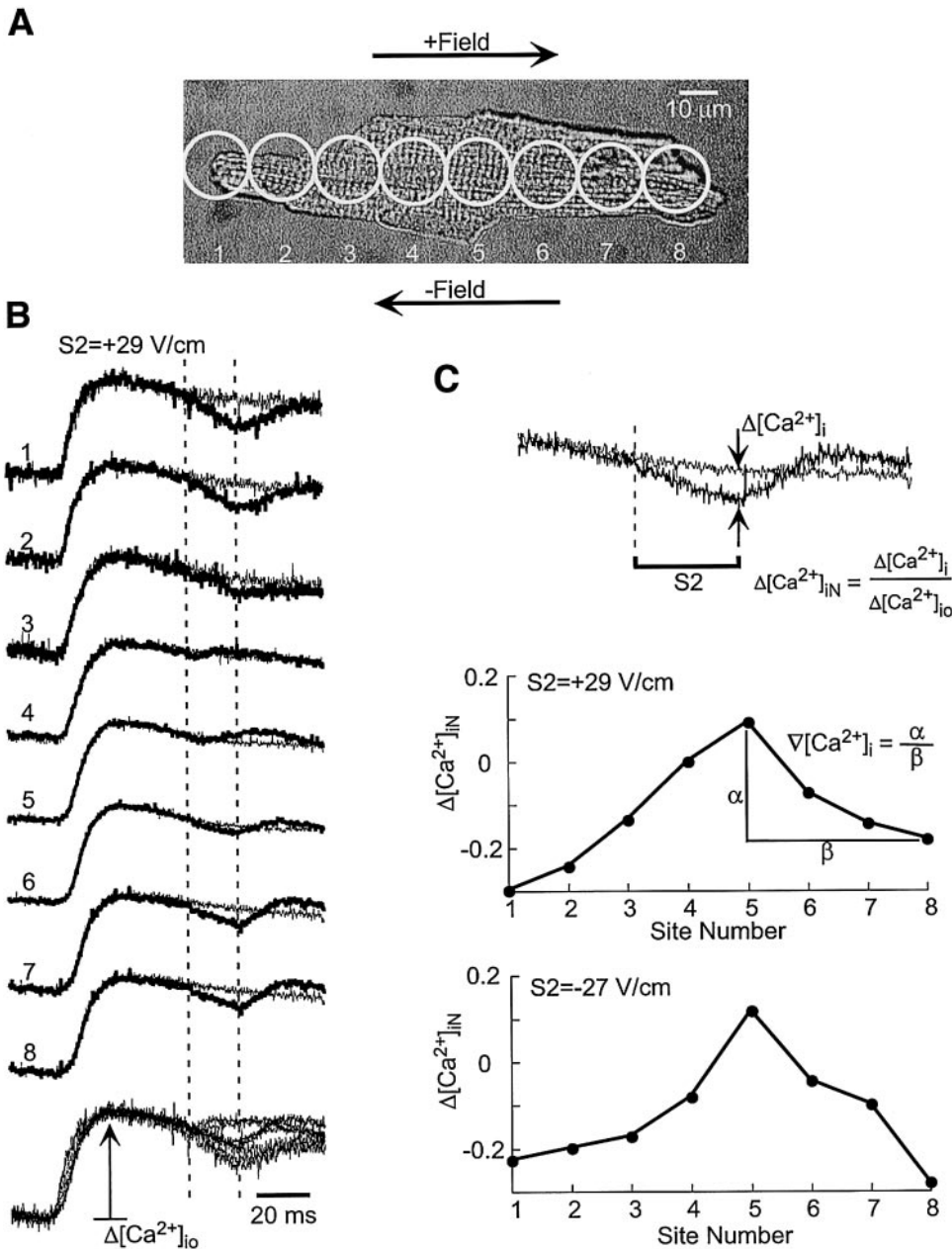


Fig. 5. Effect of S2 pulse. A: cell that was first stimulated with an S1 pulse only and then with a pair of S1-S2 pulses. $[\text{Ca}^{2+}]_i$ recordings obtained from 8 sites in response to the S1 pulse and S1-S2 pair are shown superimposed for each site in B. B: bottommost row shows the $[\text{Ca}^{2+}]_i$ transients superimposed from all sites in response to the S1-S2 pair. The pair of vertical dashed lines represents duration of S2 pulse. Perturbation of the $[\text{Ca}^{2+}]_i$ transients was measured at the end of S2 pulse with respect to the value of $[\text{Ca}^{2+}]_i$ recorded with the S1 pulse only as illustrated in inset of C. Change was normalized to $\Delta[\text{Ca}^{2+}]_{i0}$ and is plotted against the site number in C, top. C, bottom shows $\Delta[\text{Ca}^{2+}]_{iN}$ for the same cell in response to an S1-S2 pair applied in the negative direction (S2 = -27 V/cm). For both field directions $\Delta[\text{Ca}^{2+}]_{iN}$ was smallest at the cell center and increased in either direction implying that $\nabla[\text{Ca}^{2+}]_i$ developed directed from the cell center to both cell ends. For +29 V/cm S2 pulse (C, top) $\nabla[\text{Ca}^{2+}]_i$ values were found to be 5.6 and 5.2 nM/ μm for the anodal and cathodal halves of the cell, respectively. For -27 V/cm S2 pulse (C, bottom) $\nabla[\text{Ca}^{2+}]_i$ values were found to be 7.7 and 5.0 nM/ μm , respectively.

polarization becomes superimposed on the upstroke of the action potential. Hence, the hyperpolarization at the anodal end could significantly increase the driving force for influx of Ca^{2+} and compensate for the smaller activation of the Ca^{2+} channel, producing a larger and faster $[\text{Ca}^{2+}]_i$ transient at the anodal end. Another explanation for our experimental results could involve voltage-dependent inactivation of the L-type Ca^{2+} channels, which exists to some extent in guinea pig ventricular cells (16, 31). Assuming that the action potential is elicited during the S1 pulse, the hyperpolarization at the anodal end could diminish the inactivation of the Ca^{2+} channels compared with the cathodal end, so that upon S1 termination a larger influx of Ca^{2+} occurs at the anodal end. A third possibility involves Ca^{2+} -dependent inactivation of the L-

type Ca^{2+} channels (12). During the S1 pulse, calcium could be brought into the cell in the depolarized regions and extruded from the hyperpolarized regions of the cell via the electrogenic $\text{Na}^+/\text{Ca}^{2+}$ exchanger. This would result in a graded calcium concentration along the cell length in the restricted subspace and at the inner face of the cell membrane. The net effect would be to accentuate inactivation in the depolarized regions, and if Ca^{2+} conductance were partially inactivated at rest via calcium-dependent inactivation, to relieve inactivation in the hyperpolarized regions of the cell. Thus there would exist a spatially varying Ca^{2+} conductance along the cell length that could explain the observed S1-induced pattern of calcium transients.

Similar to the S1 pulse, the S2 pulse also causes hyperpolarization of the anodal-facing end and depo-

larization of the cathodal-facing end of the cell. However, unlike S1, this perturbation occurs from about the center (~ 10 mV) of the I - V relation for Ca^{2+} current when the S1-S2 delay is 50 ms. Thus Ca^{2+} current and $[\text{Ca}^{2+}]_i$ are expected to decrease at both ends of the cell compared with the center, as is the case experimentally (Fig. 5B). Upon S2 termination, the transmembrane potential returns close to the prepulse plateau level, resulting in a large inward Ca^{2+} current and surge in $[\text{Ca}^{2+}]_i$ at both ends of the cell (Fig. 5B, sites 1, 2, 7, and 8). The deactivation of Ca^{2+} channels at the anodal end and associated reduction in the channel conductance may explain the smaller amplitude of $[\text{Ca}^{2+}]_i$ surge in the anodal regions. We found the S2-induced $\nabla[\text{Ca}^{2+}]_i$ in the anodal regions of the cell to be greater than in the cathodal regions (Fig. 5C). Such differences are possible if the I - V relation of the Ca^{2+} current is not symmetric about the peak of the bell. Indeed, several different investigators have reported I - V relations that are slightly asymmetric with a larger slope for the negative potentials (15, 22, 29). Such an asymmetry will produce a larger spatial gradient in Ca^{2+} current and therefore in $[\text{Ca}^{2+}]_i$ in the anodal half of the cell. Another possibility is that an enhanced activity of the $\text{Na}^+/\text{Ca}^{2+}$ exchanger at the negative transmembrane potentials results in greater extrusion of Ca^{2+} from the hyperpolarized regions of the cell. This would result in greater depression of $[\text{Ca}^{2+}]_i$ and accentuation of $\nabla[\text{Ca}^{2+}]_i$ in the hyperpolarized regions compared with the depolarized regions.

It is worthwhile mentioning that the pattern of $\nabla[\text{Ca}^{2+}]_i$ would most likely be altered if the S2 pulse were to be applied during a later phase of the action potential, e.g., during the early repolarizing phase. Now the field-induced perturbation in transmembrane potential (V_m) would occur about a prepulse potential that is more negative than the early plateau value of ~ 10 mV. Thus the pattern of field-induced change in inward Ca^{2+} current, and therefore that of $[\text{Ca}^{2+}]_i$, should be different. For example, if the prepulse potential is at the midpoint of the left half of the bell-shaped I - V relation of the Ca^{2+} current, then the field-induced changes in $[\text{Ca}^{2+}]_i$ are expected to vary monotonically along the cell length with hyperpolarized regions undergoing a decrease in $[\text{Ca}^{2+}]_i$ and depolarized regions undergoing an increase in $[\text{Ca}^{2+}]_i$.

The existence of field-induced gradients in $[\text{Ca}^{2+}]_i$ is consistent with the notion that the diffusion of intracellular Ca^{2+} is a relatively slow process. If the Ca^{2+} diffusion were rapid, we should have observed smoothing of calcium gradients with time (e.g., during the S2 pulse). Indeed, several other studies directly or indirectly suggest that Ca^{2+} diffusion in cardiac tissue is severely retarded (3, 17, 27), although accurate quantitative estimates of diffusion constant (D) are unavailable. However, the value of D has been measured for skeletal muscle and is estimated to be $14 \mu\text{m}^2/\text{s}$ (20). Allbritton et al. (1) measured a similar value of D ($\sim 38 \mu\text{m}^2/\text{s}$) in the cytosol extract from *Xenopus* oocytes and attributed the slow diffusion to abundance of Ca^{2+} -buffering proteins in their extract. Because cardiac

muscle, too, has plentiful Ca^{2+} buffers (e.g., inner sarcolemma, outer SR, troponin C, mitochondria, calmodulin), a slow diffusion of Ca^{2+} is not surprising. Assuming a conservatively high value for intracellular Ca^{2+} D to be $\sim 370 \mu\text{m}^2/\text{s}$, which is the D for free Ca^{2+} in a medium with twice the viscosity of water (approximate viscosity of the cytosol) (1), the thickness of the diffusion layer s is estimated to be $\sim 6 \mu\text{m}$ [$s = (2Dt)^{0.5}$, where $t = 50$ ms is the S2 duration]. Considering that our intersite distance ($17 \mu\text{m}$) was much larger than s , the effect of diffusion in smoothing the $[\text{Ca}^{2+}]_i$ gradients is expected to be small.

Because we were primarily interested in the field-induced changes in $[\text{Ca}^{2+}]_i$, we used essentially single wavelength measurements of fluo-3 to record relative changes in $[\text{Ca}^{2+}]_i$, and for technical reasons, we did not use the more complex ratiometric method that potentially could have yielded absolute measurements of $[\text{Ca}^{2+}]_i$. Thus our estimates of the field-induced gradients in $[\text{Ca}^{2+}]_i$ rely on an assumed value for peak $[\text{Ca}^{2+}]_i$, which was assigned a typical value reported in the literature. However, the peak $[\text{Ca}^{2+}]_i$ may vary somewhat from the assumed value and also from one cell to another, and thus produce an uncertainty in the reported field-induced $[\text{Ca}^{2+}]_i$ changes and gradients.

Finally, our field amplitudes were limited to ~ 40 V/cm. It has been reported that for higher field amplitudes when the induced V_m exceeds the electroporation threshold, the cells undergo preferential hypercontraction at the anodal end, which is hypothesized to be the result of an electroosmosis-driven Ca^{2+} influx at the anodal end (19). Under such conditions, the field-induced $[\text{Ca}^{2+}]_i$ gradients may have a different pattern than those reported in this study.

In summary, we have shown that uniform electric fields can induce spatial inhomogeneities in $[\text{Ca}^{2+}]_i$ in single cells. Because $[\text{Ca}^{2+}]_i$ regulates several sarcolemmal currents (21), an accounting for nonuniformities in $[\text{Ca}^{2+}]_i$ might be important for accurately predicting the field-induced membrane responses of single cardiac cells and presumably of cardiac tissue.

This work was supported by National Heart, Lung, and Blood Institute Grant HL-48266.

REFERENCES

1. Allbritton NL, Meyer T, and Stryer L. Range of messenger action of calcium ion and inositol 1,4,5-trisphosphate. *Science* 258: 1812–1815, 1992.
2. Barceñas-Ruiz L and Wier WG. Voltage dependence of intracellular Ca^{2+} transients in guinea pig ventricular myocytes. *Circ Res* 61: 148–154, 1987.
3. Berlin JR. Spatiotemporal changes of Ca^{2+} during electrically evoked contractions in atrial and ventricular cells. *Am J Physiol Heart Circ Physiol* 269: H1165–H1170, 1995.
4. Bers DM. Ca transport during contraction and relaxation in mammalian ventricular muscle. *Basic Res Cardiol* 92: 1–10, 1997.
5. Bers DM. Calcium fluxes involved in control of cardiac myocyte contraction. *Circ Res* 87: 275–281, 2000.
6. Bers DM. Species differences and the role of sodium-calcium exchange in cardiac muscle relaxation. *Ann NY Acad Sci* 639: 375–385, 1991.

7. **Beuckelmann DJ and Wier WG.** Mechanism of release of calcium from sarcoplasmic reticulum of guinea-pig cardiac cells. *J Physiol (Lond)* 405: 233–255, 1988.
8. **Bridge JH, Smolley JR, and Spitzer KW.** The relationship between charge movements associated with ICa and INa-Ca in cardiac myocytes. *Science* 248: 376–378, 1990.
9. **Callewaert G, Cleemann L, and Morad M.** Epinephrine enhances Ca^{2+} current-regulated Ca^{2+} release and Ca^{2+} reuptake in rat ventricular myocytes. *Proc Natl Acad Sci USA* 85: 2009–2013, 1988.
10. **Cannell MB, Berlin JR, and Lederer WJ.** Effect of membrane potential changes on the calcium transient in single rat cardiac muscle cells. *Science* 238: 1419–1423, 1987.
11. **Cheng DKL, Tung L, and Sobie EA.** Nonuniform responses of transmembrane potential during electric field stimulation of single cardiac cells. *Am J Physiol Heart Circ Physiol* 277: H351–H362, 1999.
12. **Eckert R and Chad JE.** Inactivation of Ca channels. *Prog Biophys Mol Biol* 44: 215–267, 1984.
13. **Fabiato A.** Calcium release in skinned cardiac cells: variations with species, tissues, and development. *Fed Proc* 41: 2238–2244, 1982.
14. **Fabiato A.** Simulated calcium current can both cause calcium loading in and trigger calcium release from the sarcoplasmic reticulum of a skinned canine cardiac Purkinje cell. *J Gen Physiol* 85: 291–320, 1985.
15. **Grantham CJ and Cannell MB.** Ca^{2+} influx during the cardiac action potential in guinea pig ventricular myocytes. *Circ Res* 79: 194–200, 1996.
16. **Hadley RW and Lederer WJ.** Ca^{2+} and voltage inactivate Ca^{2+} channels in guinea-pig ventricular myocytes through independent mechanisms. *J Physiol (Lond)* 444: 257–268, 1991.
17. **Isenberg G, Etter EF, Wendt-Gallitelli MF, Schiefer A, Carrington WA, Tuft RA, and Fay FS.** Intracellular $[\text{Ca}^{2+}]$ gradients in ventricular myocytes revealed by high speed digital imaging microscopy. *Proc Natl Acad Sci USA* 93: 5413–5418, 1996.
18. **Josephson IR, Sanchez-Chapula J, and Brown AM.** A comparison of calcium currents in rat and guinea pig single ventricular cells. *Circ Res* 54: 144–156, 1984.
19. **Knisley SB and Grant AO.** Asymmetrical electrically induced injury of rabbit ventricular myocytes. *J Mol Cell Cardiol* 27: 1111–1122, 1995.
20. **Kushmerick MJ and Podolsky RJ.** Ionic mobility in muscle cells. *Science* 166: 1297–1298, 1969.
21. **Luo CH and Rudy Y.** A dynamic model of the cardiac ventricular action potential. I. Simulations of ionic currents and concentration changes. *Circ Res* 74: 1071–1096, 1994.
22. **Rose WC, Balke CW, Wier WG, and Marban E.** Macroscopic and unitary properties of physiological ion flux through L-type Ca^{2+} channels in guinea-pig heart cells. *J Physiol (Lond)* 456: 267–284, 1992.
23. **Santana LF, Cheng H, Gomez AM, Cannell MB, and Lederer WJ.** Relation between the sarcolemmal Ca^{2+} current and Ca^{2+} sparks and local control theories for cardiac excitation-contraction coupling. *Circ Res* 78: 166–171, 1996.
24. **Sharma V and Tung L.** Transmembrane responses of single guinea pig myocyte to uniform electric field stimulus. *J Cardiovasc Electrophysiol* 10: 1296, 1999.
25. **Sipido KR, Maes M, and Van de Werf F.** Low efficiency of Ca^{2+} entry through the Na^{+} - Ca^{2+} exchanger as trigger for Ca^{2+} release from the sarcoplasmic reticulum. A comparison between L-type Ca^{2+} current and reverse-mode Na^{+} - Ca^{2+} exchange. *Circ Res* 81: 1034–1044, 1997.
26. **Sipido KR and Wier WG.** Flux of Ca^{2+} across the sarcoplasmic reticulum of guinea pig cardiac cells during excitation contraction coupling. *J Physiol (Lond)* 435: 605–630, 1991.
27. **Takamatsu T and Wier WG.** Calcium waves in mammalian heart: quantification of origin, magnitude, waveform and velocity. *FASEB J* 4: 1519–1525, 1990.
28. **Takamatsu T and Wier WG.** High temporal resolution video imaging of intracellular calcium. *Cell Calcium* 11: 111–120, 1990.
29. **Varro A, Lathrop DA, Hester SB, Nanasi PP, and Papp JG.** Ionic currents and action potentials in rabbit, rat, and guinea pig ventricular myocytes. *Basic Res Cardiol* 88: 93–102, 1993.
30. **Watanabe T, Rautaharju PM, and McDonald TF.** Ventricular action potentials, ventricular extracellular potentials, and the ECG of guinea pig. *Circ Res* 57: 362–373, 1985.
31. **White E and Terrar DA.** Inactivation of Ca current during the action potential in guinea-pig ventricular myocytes. *Exp Physiol* 77: 153–164, 1992.
32. **Windisch H, Ahammer H, Schaffer P, Muller W, and Platzer D.** Optical multisite monitoring of cell excitation phenomena in isolated cardiomyocytes. *Pflügers Arch* 430: 508–518, 1995.